# Valence Electron Distribution in Cubic Tetracyanoethylene by the Combined Use of X-Ray and Neutron Diffraction[1a]

**P. Becker,[1b] P. Coppens,*[1b] and F. K. Ross[1c]**

*Contribution from the Chemistry Departments, State University of New York at Buffalo, Buffalo, New York 14214, and Brookhaven National Laboratory, Upton, Long Island, New York 11973.* *Received April 3, 1973*

**Abstract:** An earlier X-ray diffraction analysis on cubic tetracyanoethylene has been complemented by a neutron diffraction study. The neutron diffraction results confirm that X-ray positional parameters are affected by the asphericity shift, which results from the assumption of spherical atomic symmetry in the X-ray refinement. The neutron diffraction bond lengths are in good agreement with the results of an earlier double-atom refinement of the X-ray data, though the asphericity shift is largest for the cyano carbon, rather than the nitrogen atom, as followed from the earlier treatment. Neutron thermal parameters are on the average 13% lower than the corresponding X-ray values, indicating systematic errors introduced by the spherical atom model. X–N difference density maps show pronounced overlap and lone pair density peaks. The highest of these is in the C≡N bond and exceeds 12 times the estimated standard deviation in the density. The results are in qualitative agreement with the Hartree–Fock difference density of dicyanogen, except in the lone pair region which appears significantly lower in the experimental maps.

A number of studies have appeared in the last few years in which X-ray and neutron diffraction techniques have been combined to obtain a measure of the redistribution of the valence electrons upon molecule formation.[2–6] From these studies it has become evident that information of chemical interest can be extracted. For example, the lone pair density can be readily recognized, the overlap density in pure $\sigma$ bonds differs from the density in bonds having $\pi$ character, and the bond density in a three-membered ring compound peaks outside the triangle defined by the nuclear positions.[6]

Tetracyanoethylene is a molecule of interest, because it contains three distinctly different bonds, which can be loosely described as being triple, double, and single bonds. The crystal structure of the cubic modification is simple and has been studied recently in our laboratory.[7,8a] The present study is a complementary neutron diffraction investigation and an analysis of the combined data sets in terms of the bonding electron distribution. The results are compared with those of theoretical calculations on dicyanogen[8b] and with the experimental results on tetracyanoethylene oxide,[6a] which is the only other cyano compound that has been studied by the combined X-ray and neutron diffraction technique.

## Experimental Section

Crystals of cubic tetracyanoethylene (TCNE) were grown from ethyl acetate solutions. The form {100} was developed. A crystal of dimensions 2.1 × 2.6 × 3.2 mm parallel to *a*, *b*, and *c*, respectively, was selected. Crystallographic information as determined by X-rays[7] is given in Table I. Data were collected at the Brookhaven high-flux beam reactor. A first data set was discarded because of unsatisfactory fit between symmetry-equivalent reflections. The second data set contained 1467 reflections with $\sin \theta/\lambda < 0.68$ Å$^{-1}$, which were subsequently averaged to give 508 unique reflections. The internal consistency $R$ factor $\Sigma|F^2 - \langle F^2\rangle|/\Sigma F^2$ was 3.5% and reduced to 3.3% when weighting was introduced based on counting statistics. The data were refined by least squares, including anisotropic extinction in the Zachariasen approximation.[9] The neutron scattering length for carbon was taken as $0.665 \times 10^{-12}$ cm,[10] while the revised value of $0.913 \times 10^{-12}$ cm[11] was selected for nitrogen. Both type I and type II models were applied in the extinction refinement with very similar results. However, extinction in the neutron data is quite severe, 12 reflections having an extinction factor $y < 0.2$, the lowest of which is 0.12. It is, therefore, more likely that the mosaic domain is large, which implies that extinction is mosaic spread dominated (type I crystal). Information on the experiment and the data refinement is summarized in Table II. Final parameters (anisotropic type I only) are given in Table III. A list of observed and calculated neutron structure factors is given in Table IV (see the paragraph at the end of the paper regarding supplementary material).

**Table I.** Crystallographic Information[7]

| | |
|---|---|
| Space group | *Im*3 |
| *a* | 9.736 ± 0.006 Å |
| *Z* | 6 |
| Point group symmetry of the molecules | $2/m2/m2/m$ ($D_{2h}$) |

## Atomic Coordinates

Due to the high symmetry of the site occupied by the TCNE molecule, the structure is fully described by only five variable parameters, listed in Table IV, together with the bond lengths (Figure 1). It was realized in earlier work[7,8a] that at the high precision of the X-ray analysis noncoincidence of the nuclear positions and

---

(1) (a) Research performed in part under the auspices of the U. S. Atomic Energy Commission. (b) University of New York at Buffalo. (c) Brookhaven National Laboratory.

(2) P. Coppens, *Science*, **158**, 1577 (1967).

(3) P. Coppens, T. M. Sabine, R. G. Delaplane, and J. A. Ibers, *Acta Crystallogr., Sect. B*, **25**, 2451 (1969).

(4) J. C. Taylor and T. M. Sabine, *Acta Crystallogr., Sect. B*, **28**, 3340 (1972).

(5) P. Coppens and A. Vos, *Acta Crystallogr., Sect. B*, **27**, 146 (1971).

(6) (a) D. A. Matthews and G. D. Stucky, *J. Amer. Chem. Soc.*, **93**, 5954 (1971). (b) D. A. Matthews, G. D. Stucky, and P. Coppens, *J. Amer. Chem. Soc.*, **94**, 8001 (1972).

(7) R. G. Little, D. Pautler, and P. Coppens, *Acta Crystallogr., Sect. B*, **27**, 1493 (1971).

(8) (a) P. Coppens, *Acta Crystallogr., Sect. B*, **27**, 1931 (1971); (b) F. L. Hirshfeld, *ibid.*, **27**, 769 (1971).

(9) P. Coppens and W. C. Hamilton, *Acta Crystallogr., Sect. A*, **26**, 71 (1970).

(10) The Neutron Diffraction Commission, *Acta Crystallogr., Sect. A*, **25**, 391 (1969).

(11) W. C. Hamilton, private communication; "Neutron Cross Sections," BNL 325, Brookhaven National Laboratory, 1964.

Table II. Details on Neutron Diffraction Analysis

| | |
|---|---|
| Wavelength | λ 1.014 Å |
| No. of observations (after averaging) | 503 |
| No. of variables | 23 |
| Refinement based on $F^2$, $\sigma^2(F^2) = \sigma^2_{\text{counting}} + (0.05F^2)^2$ | |
| Isotropic extinction | $R(F^2) = \dfrac{\Sigma\lvert F_o^2 - k^2F_c^2\rvert}{\Sigma F_o^2} = 0.034$ |
| | $R_w(F^2) = \left\{\dfrac{\Sigma w(F_o^2 - k^2F_c^2)^2}{\Sigma wF_o^4}\right\}^{1/2} = 0.043$ |
| Anisotropic extinction (type I) | |
| | $R(F^2) = 0.027$ |
| | $R_w(F^2) = 0.034$ |

Table III. Results of Neutron and X-Ray Analyses[a]

| | | Neutron (type I) | X-Ray |
|---|---|---|---|
| N(1) | $x$ | 0.21294 (6) | 0.21288 (12) |
| | $z$ | 0.72182 (6) | 0.72162 (10) |
| | $U_{11}$ | 0.0451 (4) | 0.0507 (7) |
| | $U_{22}$ | 0.0453 (4) | 0.0479 (6) |
| | $U_{33}$ | 0.0300 (4) | 0.0403 (6) |
| | $U_{13}$ | −0.0139 (2) | −0.0094 (4) |
| C(2) | $x$ | 0.14714 (6) | 0.14765 (11) |
| | $z$ | 0.62436 (6) | 0.62488 (11) |
| | $U_{11}$ | 0.0311 (4) | 0.0346 (6) |
| | $U_{22}$ | 0.0306 (4) | 0.0319 (5) |
| | $U_{33}$ | 0.0239 (4) | 0.0299 (6) |
| | $U_{13}$ | −0.0039 (2) | 0.0009 (4) |
| C(1) | $x$ | 0.0696 (8) | 0.0690 (15) |
| | $U_{11}$ | 0.0277 (5) | 0.0355 (8) |
| | $U_{22}$ | 0.0254 (5) | 0.0253 (6) |
| | $U_{33}$ | 0.0195 (5) | 0.0257 (7) |
| Extinction | $G_{11}$ | 191 (14) | |
| | $G_{22}$ | 106 (7) | |
| | $G_{33}$ | 158 (19) | |
| | $G_{12}$ | 59 (13) | |
| | $G_{23}$ | 10 (12) | |
| | $G_{13}$ | 5 (12) | |

[a] Fractional coordinates, mean square thermal displacement tensors (in Å$^2$), and mosaic spread parameters (×10$^4$).

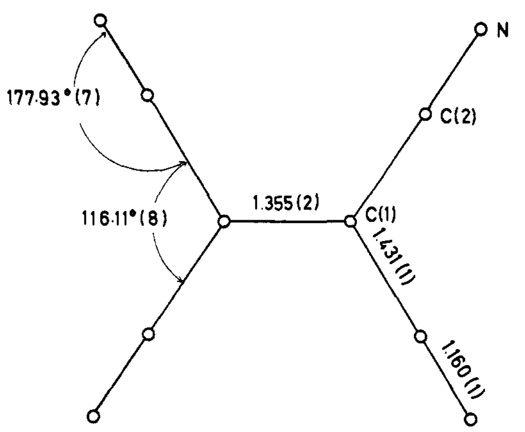

Figure 1. Bond lengths (corrected for thermal motion according to the riding model) and angles in the TCNE molecule according to the neutron diffraction analysis.

Table IV. Atomic Coordinates and Bond Lengths (Corrected for Thermal Motion) (Å)[a]

| | | | X-Ray double-atom refinement | | |
|---|---|---|---|---|---|
| | X-Ray | Neutron | Core | Valence shell | Electron diffraction[12] |
| N | | | | | |
| $x$ | 2.073 (1) | 2.073 (1) | 2.077 (1) | 2.044 (5) | |
| $y$ | 4.868 | 4.868 | 4.868 | 4.868 | |
| $z$ | 7.025 (1) | 7.027 (1) | 7.034 (1) | 6.989 (5) | |
| C(2) | | | | | |
| $x$ | 1.438 (1) | 1.432 (1) | 1.435 (1) | 1.438 (6) | |
| $y$ | 4.868 | 4.868 | 4.868 | 4.868 | |
| $z$ | 6.084 (1) | 6.078 (1) | 6.081 (1) | 6.074 (7) | |
| C(1) | | | | | |
| $x$ | 0.672 (2) | 0.677 (1) | 0.679 (2) | 0.679 (2) | |
| $y$ | 4.868 | 4.868 | 4.868 | 4.868 | |
| $z$ | 4.868 | 4.868 | 4.868 | 4.868 | |
| C(2)–N | 1.153 (2)<br>[1.135] | 1.160 (1)<br>[1.145] | 1.166 (2)<br>[1.149] | | 1.162 |
| C(1)–C(2) | 1.439 (2)<br>[1.437] | 1.431 (1)<br>[1.427] | 1.431 (2)<br>[1.429] | | 1.435 |
| C(1)–C(1)′ | 1.344 (3)<br>[1.344] | 1.355 (2)<br>[1.355] | 1.358 (3)<br>[1.358] | | 1.357 |

[a] Estimated standard deviations are given in parentheses. Absence of a standard deviation indicates coordinate fixed by symmetry. Bond lengths in square brackets are before correction for thermal motion shortening.

the centroids of the charge density may not be negligible relative to the experimental standard deviations. Significant differences between X-ray and neutron positional parameters in a number of other compounds have been attributed to bonding effects on the electron density.[3] To assess the "asphericity shift" from X-ray data alone, a double atom refinement method[8a] was developed in which the atomic valence shell is allowed to float with respect to the core electrons in the course of the least-squares refinement of the structure factors. Results of both the conventional X-ray refinement and the double-atom method have been added to Table IV. It is to be noted that differences between the X-ray and neutron values are larger than 3$\sigma$ for the C(1)–C(1)′ bond across the center of symmetry. In each case the internuclear distances as derived from the double-atom refinement method are in better agreement with the neutron values than the conventional X-ray values. Furthermore, as may be expected, the neutron diffraction and "double-atom" bond lengths agree better with the electron diffraction values given by Hope.[12]

When the positional parameters rather than the bond lengths are compared, it becomes apparent that the discrepancies, though small, are largest for the cyano group carbon atom, the X-ray atom being displaced by about 0.0085 (15) Å toward the nitrogen atom. This is in agreement with model calculations of the asphericity shift by Matthews and Stucky,[6a] which gave values of 0.032 and 0.003 Å for C and N, respectively (both shifts are in the direction fo the C–N vector). It has been observed before[3] that the model calculations overestimate the size of the shift, but the larger shift of the carbon atom and its direction are properly predicted. The shift of the carbon centroid is attributable to the overlap density in the triple bond being larger than the density in the single C–C bond. The nitrogen atom density, more evenly distributed as the long pair, and C≡N overlap density have approximately equal and opposing contributions to the atomic dipole moment.[6a]

In tetracyanoethylene oxide (TCEO) the X-ray–neutron differences were somewhat random for the nitrogen atoms of the four crystallographically in-

---

[12] H. Hope, *Acta Chem. Scand.*, 22, 1057 (1968).

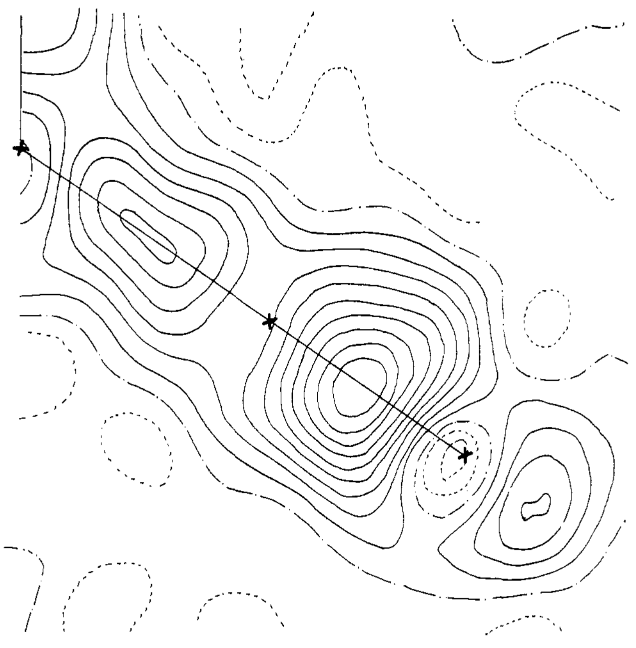

Figure 2. Section in the molecular plane showing the function $\Delta\rho_{X-N}$. Contours at each 0.10 Å$^{-3}$: negative contours (---); zero contour (-···). The cross to the right indicates the position of the nitrogen atom. The carbon atoms are to the left.

dependent C≡N groups and toward the nitrogen for three of the four cyano carbon atoms. Thus, the *average* shifts in TCEO are in qualitative agreement with the present results, which supports the explanation given[6a] that the spuriousness of the nitrogen shifts in TCEO is due to systematic errors in the data.

It is worthwhile noting that the success of the double-atom refinement in predicting the neutron C≡N bond length is mainly due to a shift of the nitrogen core position. Thus, while the method has lead to good internuclear separations, the location of the core electrons may not strictly correspond to the nuclear positions. This deviation should be attributed to the shortcomings of the spherical approximation for the valence electrons made in the double-atom formalism.

## Thermal Parameters

The X-ray thermal parameters (refinement based on $F^2$) are given for comparison purposes in Table III. As observed in previous studies,[13] the X-ray thermal parameters are larger than the neutron values, indicating the effect of using isolated-atom form factors in the X-ray refinement of a molecular crystal. In TCNE the differences in the $U_{ii}$ mean-square displacement tensors range from very slightly negative (for $U_{22}$ of C(1)) to 0.010 Å$^2$ ($U_{33}$ of N), the average deviation being 0.0048 Å$^2$ or 13% of the average X-ray $U_{ii}$ value. These discrepancies are similar to those observed earlier.[13]

## X-N Difference Density Maps

**Estimate of Errors and Interpretation.** Bonding features in electron density maps are not readily apparent from X-ray data alone, because the X-ray parameters are adjusted in the least-squares refinement such as to partially allow for bonding asymmetry. The resulting discrepancies between X-ray and neutron parameters were discussed above. The redistribution of the electron density on molecule formation can be

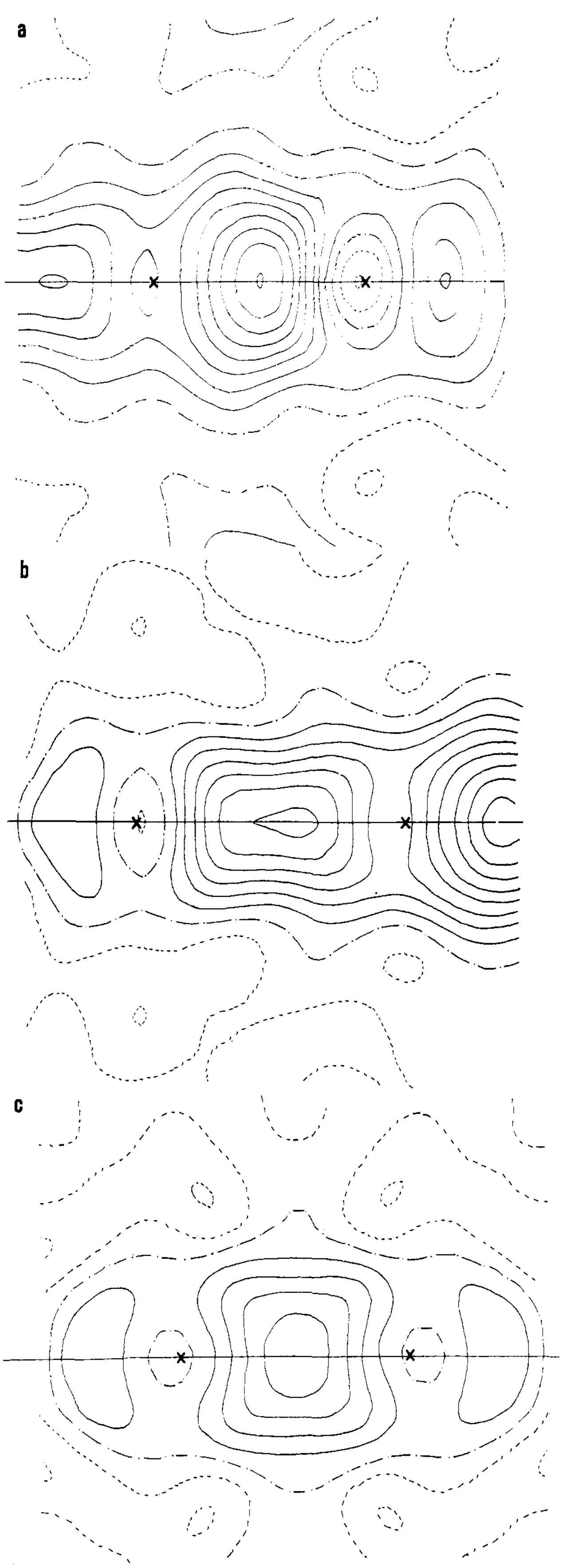

Figure 3. Sections perpendicular to the molecular plane through bonds: (a) through C≡N; (b) through C=C; (c) through C—C. Contours as in Figure 2.

---

[13] P. Coppens, *Acta Crystallogr., Sect. B*, 24, 1272 (1968).

obtained from the function

$$\Delta\rho_{\text{X-N}}(\mathbf{r}) = \rho_{\text{X}} - \rho_{\text{N}} = \frac{1}{V}\sum_i (F_{\text{X}} - F_{\text{N}})\cos(2\pi\mathbf{H}_i\cdot\mathbf{r}) \quad (1)$$

applicable when the origin coincides with a crystallographic center of symmetry. Here, $\mathbf{H}_i$ is a reciprocal lattice vector, $\mathbf{r}$ describes a point in the crystal space, $V$ is the volume of the unit cell, $F_{\text{X}}$ is the X-ray structure factor with calculated sign, and $F_{\text{N}}$ is defined by

$$F_{\text{N}}(\mathbf{H}) = \sum_i f_i \cos(2\pi\mathbf{H}\cdot\mathbf{r}_{i,\text{N}})T_{i,\text{N}} \quad (2)$$

where $r_{i,\text{N}}$ and $T_{i,\text{N}}$ are the neutron positional parameters and temperature factors respectively, and $f_i$ is the isolated atom X-ray from factor.

Figures 2–4 represent a series of sections through various parts of the molecule of the function $\Delta\rho_{\text{X-N}}$. It is apparent that the value of the difference density is very small in regions remote from the atomic positions, indicating the reasonable quality of the data, while very distinct features of appreciable height are found between the atoms and at the back of the nitrogen atom, in what may be loosely described as the nitrogen lone pair region. The highest peak is at the center of the triple bond and reaches 0.9 Å$^{-3}$.

It is of interest to obtain an estimate of the standard deviation in this difference density. We have

$$\sigma^2(\Delta\rho_{\text{X-N}}) = \sigma^2(\rho_{\text{X}}) + \sigma^2(\rho_{\text{N}}) = \frac{1}{V^2}[\Sigma\sigma^2(F_{\text{X}}) \times \cos^2(2\pi\mathbf{H}_i\cdot\mathbf{r}) + \Sigma\sigma^2(F_{\text{N}})\cos^2(2\pi\mathbf{H}_i\cdot\mathbf{r})] \quad (3)$$

Since the contribution of the terms in the summation depends on the value of $\mathbf{H}\cdot\mathbf{r}$, the error function varies within the unit cell.[14] However, following Cruickshank[15] the average error in the density may be estimated from

$$\sigma^2(\rho_{\text{X}}) \approx \sum_{\substack{\text{all ob-}\\\text{servations}}} \sigma^2(F_{\text{X}})$$

if series termination errors are ignored. For tetracyanoethylene the average error is estimated as 0.05 Å$^{-3}$, using standard deviations in the structure factors $F$ based on counting statistics and an error proportional to the magnitude of $F$.[7]

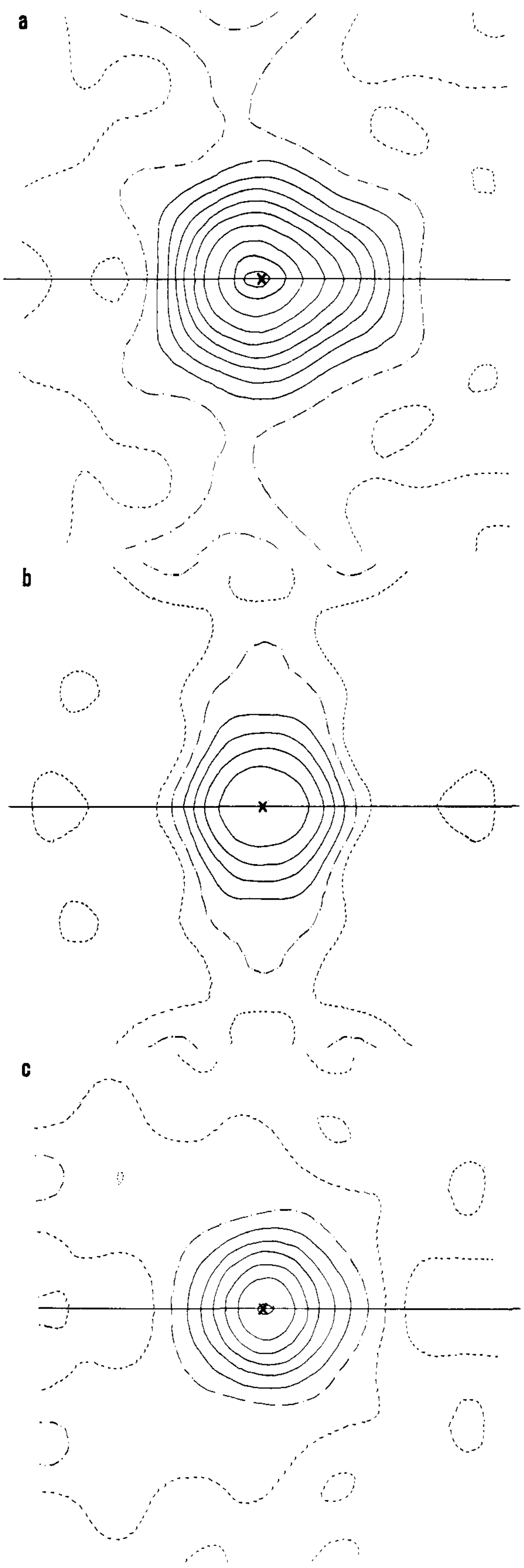

Figure 4. Sections are perpendicular to bonds through midpoints of bonds: (a) perpendicular to C≡N; (b) perpendicular to C═C; (c) perpendicular to C—C. Contours as in Figure 2. The straight lines indicate the intersection with the plane of the molecule.

The error in $\rho_{\text{N}}$ is more difficult to assess. It occurs as a result of the experimental uncertainties in the neutron parameters $r_{i,\text{N}}$ and $T_{i,\text{N}}$ in (2) and is related to the error in $\rho_{\text{nuclear}}$, the nuclear neutron scattering density. In the same approximation used above one gets

$$\sigma^2(\rho_{\text{nuclear}}) \approx \sum_{\substack{\text{all ob-}\\\text{servations}}} \sigma^2(F_{\text{nuclear}})$$

where $F_{\text{nuclear}}(\mathbf{H}) = \Sigma_i = b_i\cos(2\pi\mathbf{H}r_{i,\text{N}})$ and $b_i$ is the nuclear scattering length for thermal neutrons. It follows that

$$\sigma^2(\rho_{\text{N}}) \approx \langle f_i/b_i\rangle^2\sigma^2(\rho_{\text{nuclear}})$$

Typical values for TCNE are $b_i = 0.8 \times 10^{-12}$ cm and $f_i = 3$ electrons $\approx 0.9 \times 10^{-12}$ cm. Thus, the scattering factor ratio is close to 1 and $\sigma^2(\rho_{\text{N}}) \approx \sigma^2\cdot(\rho_{\text{nuclear}}) \approx \sigma^2(\rho_{\text{X}})$ as the observations in the X-ray

---

(14) P. Coppens and W. C. Hamilton, *Acta Crystallogr., Sect. B*, **24**, 925 (1968).

(15) D. W. J. Cruickshank, *Acta Crystallogr.*, **2**, 65 (1949).

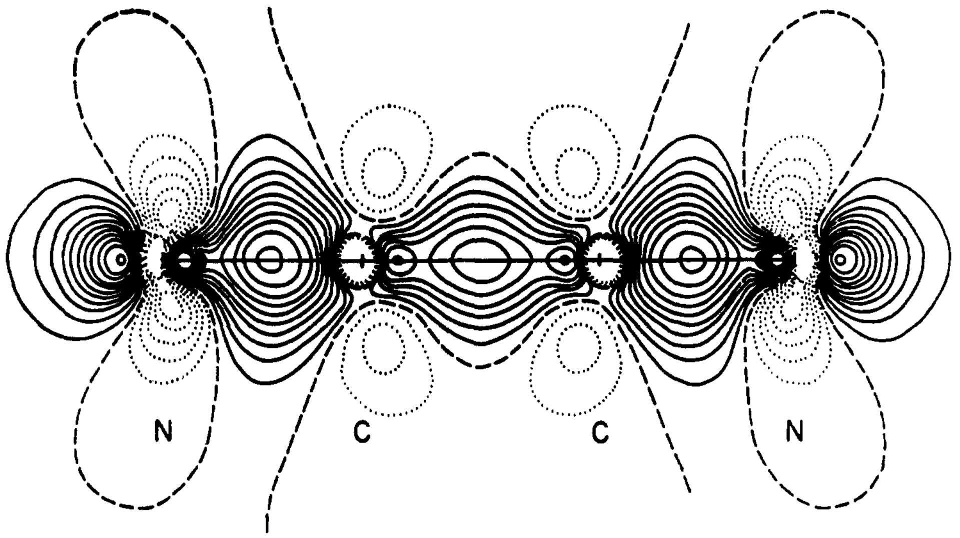

Figure 5. Theoretical difference density in NCCN as calculated by Hirshfeld.[8b] Contours at 0.1 Å$^{-3}$. Negative contours dotted.

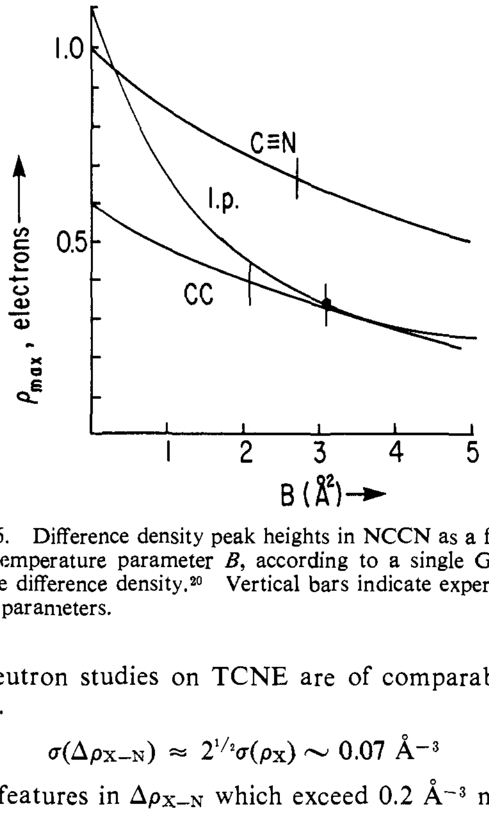

Figure 6. Difference density peak heights in NCCN as a function of the temperature parameter $B$, according to a single Gaussian fit to the difference density.[20] Vertical bars indicate experimental thermal parameters.

and neutron studies on TCNE are of comparable accuracy.

$$\sigma(\Delta\rho_{X-N}) \approx 2^{1/2}\sigma(\rho_X) \sim 0.07 \text{ Å}^{-3}$$

Thus, features in $\Delta\rho_{X-N}$ which exceed 0.2 Å$^{-3}$ may be significant. An examination of the background level of the difference density in remote areas indicates that this estimate is quite realistic, the largest negative troughs being about 0.2 Å$^{-3}$. Nevertheless, it should be kept in mind that this estimate constitutes an average error. It has been pointed out, for example, that small errors in temperature parameters introduce a large bias in the electron density in regions very close to the nuclei.[16] Hence, we shall exclude the density in the immediate vicinity of the nuclei from our discussion.

The respective heights of the overlap density in the single, double, and triple bond are 0.6, 0.4, and 0.9 Å$^{-3}$ (the difference density may be lower in a double than in a single bond, because the atoms subtracted are closer to the bond center) (Figure 2). In comparison the theoretical difference density in the molecule of dicyanogen at rest calculated by Hirshfeld[8b] from a Hartee–Fock wave function of Yoshimine and McLean[17] gives peak densities of 1.0 and 0.6 Å$^{-3}$ for the triple and single bond (Figure 5), in good qualitative agreement with the present results.

The experimental peak height of the nitrogen lone pair is 0.4 Å$^{-3}$, significantly lower than the theoretical molecule value of 1.1 Å$^{-3}$.

The proper comparison of the experimental density is with the thermally averaged theoretical difference maps.[18] A one-parameter Gaussian fit to the difference density peaks in Figure 5 allows an approximate evaluation of the effect of thermal averaging.[19] The results given in Figure 6 indicate that the sharper lone pair feature is reduced to a much greater extent than the bond density. Thus, the relatively low peak height in the lone pair region does not constitute a discrepancy with theory but is a result of the thermal smearing of the experimental density.

Cross sections perpendicular to the bonds through their midpoints are given in Figure 4. It appears that the ethylenic bond is somewhat extended in a direction perpendicular to the molecular plane, while the single bond is cylindrically symmetric and the triple bond is somewhat extended in the molecular plane. The first two observations agree with chemical considerations, while the last would indicate a bending of the triple bond. However, in view of the small size of these distortions relative to the experimental standard deviation, further discussion seems unwarranted at this time.

**Acknowledgments.** This research was supported by the National Science Foundation and by the donors of the Petroleum Research Fund, administered by the American Chemical Society. We would like to thank Dr. J. M. Williams of Argonne National Laboratory for the collection of some supplementary intensity data on TCNE.

---

(16) R. F. Stewart, *Acta Crystallogr., Sect. A*, **24**, 497 (1968).

(17) A. D. McLean and M. Yoshimine, "Tables of Linear Molecule Wave Functions," International Business Machine Corporation, San Jose, Calif., 1967.

(18) J. W. McIver, P. Coppens, and D. Nowack, *Chem. Phys. Lett.*, **11**, 82 (1971).

(19) P. Coppens, *Acta Crystallogr.*, in press.

**Supplementary Material Available.** A listing of structure factors will appear following these pages in the microfilm edition of this volume of the journal. Photocopies of the supplementary material from this paper only or microfiche (105 × 148 mm, 20× reduction, negatives) containing all of the supplementary material for the papers in this issue may be obtained from the Journals Department, American Chemical Society, 1155 16th St., N.W., Washington, D. C. 20036. Remit check or money order for $3.00 for photocopy or $2.00 for microfiche, referring to code number JACS-73-7604.

---

# Ion-Polar Molecule Collisions. The Effect of Molecular Size on Ion-Polar Molecule Rate Constants

**Timothy Su and Michael T. Bowers***

*Contribution from the Department of Chemistry, University of California, Santa Barbara, California 93106.* *Received April 30, 1973*

**Abstract:** Proton transfer rate constants from $CH_5^+$ to $CH_3Cl$, $C_2H_5Cl$, $n$-$C_3H_7Cl$, $n$-$C_4H_9Cl$, $n$-$C_5H_{11}Cl$, $i$-$C_3H_7Cl$, $i$-$C_4H_9Cl$, $t$-$C_4H_9Cl$, and $t$-$C_5H_{11}Cl$ have been measured experimentally at thermal energies by ion cyclotron resonance techniques and compared with the average dipole orientation (ADO) theory. In all cases the reaction efficiencies are near unity. The dipole moments of all of the compounds are very similar. Thus, the variations in the rate constants are correlated quantitatively with the variations in the polarizability of the polar substrates. No evidence for steric hindrance of proton transfer was found.

Ion-polar molecule collisions have been an area of interest both theoretically[1-3] and experimentally.[2-4] In Langevin's ion-induced dipole theory[5] of ion-nonpolar molecule collisions, it is assumed that both the ion and molecule are point particles. The locked dipole approximation[2,3] and the trajectory calculations[1] of ion-polar molecule collisions are based on the same assumptions. The recently developed average dipole orientation (ADO) theory[6,7] for ion-polar molecule collisions also includes these assumptions. Rate constants predicted by ADO theory are in good agreement with experimental results of some selected ion-dipole systems.[6,8,9] A recent report from this laboratory[7] has also demonstrated that the point particle ADO theory provides a workable model for some selected ion-dipole collisions when the size of the ion is less than a few ångstroms in radius.

In this paper, the ADO theory will be used as a diagnostic tool to investigate the importance of molecular size and structure on the magnitude of capture rate constants. Proton transfer rate constants from $CH_5^+$ to a number of alkyl chlorides have been measured experimentally (reaction 1) where R represents $CH_3$,

$$CH_5^+ + R\text{-}Cl \longrightarrow R\text{-}ClH^+ + CH_4 \qquad (1)$$

$C_2H_5$, $n$-$C_3H_7$, $i$-$C_3H_7$, $n$-$C_4H_9$, $i$-$C_4H_9$, $t$-$C_4H_9$, $n$-$C_5H_{11}$, and $t$-$C_5H_{11}$. This group of compounds was chosen because they have similar dipole moments but different molecular sizes and configurations.

## Results

Experiments were performed at *ca.* 300°K on an icr spectrometer which has been discussed in detail elsewhere.[10,11] Rate constants were measured by the same techniques described previously.[8] The absolute accuracy of experimental rate constants is estimated to be better than ±15%. The relative values are considerably more accurate, *ca.* ±3%. Table I summarizes the thermal energy proton transfer rate constants obtained experimentally and from the ADO theory.[6,7] Rate constants calculated from the Langevin theory and locked dipole approximations are included for comparison. The last column is the ratio of experimental to ADO theoretical rate constants. The polarizabilities, $\alpha$, and dipole moments, $\mu_D$, of the alkyl chlorides are listed in Table II. (The uncertainty in $\alpha$ is *ca.* ±10% and that of $\mu_D$ is *ca.* ±5%. This uncertainty leads to a theoretical uncertainty in the rate constant of *ca.* ±5%.)

## Discussion

Theoretical ADO rate constants are in good agreement with experimental values within the theoretical and experimental uncertainty. Both the Langevin zero dipole and the locked dipole models are in marked disagreement with experiment. The experiment/ADO ratios are near unity suggesting that every capture collision leads to reaction. An important observation is that this ratio remains approximately constant despite the substantial change of the physical size and structure of the molecules. Since polarizability is a measure of

---

(1) (a) J. V. Dugan, Jr., and J. L. Magee, *J. Chem. Phys.*, **47**, 3103 (1967); (b) J. V. Dugan, Jr., J. H. Rice, and J. L. Magee, *Chem. Phys. Lett.*, **2**, 219 (1968); (c) J. V. Dugan, Jr., J. H. Rice, and J. L. Magee, *ibid.*, **3**, 323 (1969); (d) J. V. Dugan, Jr., and R. B. Canright, Jr., *ibid.*, **8**, 253 (1971); (e) J. V. Dugan, Jr., and R. W. Palmer, *ibid.*, **13**, 144 (1972); (f) J. V. Dugan, Jr., *ibid.*, **8**, 198 (1971); (g) J. V. Dugan, Jr., and R. B. Canright, Jr., *J. Chem. Phys.*, **56**, 3625 (1972).

(2) T. F. Moran and W. H. Hamill, *J. Chem. Phys.*, **39**, 1413 (1963).

(3) S. K. Gupta, E. G. Jones, A. G. Harrison, and J. J. Myher, *Can. J. Chem.*, **45**, 3107 (1967); A. S. Blair and A. G. Harrison, *ibid.*, **51**, 1645 (1973).

(4) M. T. Bowers and J. B. Laudenslager, *J. Chem. Phys.*, **56**, 4711 (1972).

(5) G. Gioumousis and D. P. Stevenson, *J. Chem. Phys.*, **29**, 294 (1958).

(6) T. Su and M. T. Bowers, *J. Chem. Phys.*, **58**, 3027 (1973).

(7) T. Su and M. T. Bowers, *Int. J. Mass Spectrom. Ion Phys.*, in press.

(8) T. Su and M. T. Bowers, *J. Amer. Chem. Soc.*, **95**, 1370 (1973).

(9) M. T. Bowers, T. Su, and V. G. Anicich, *J. Chem. Phys.*, **58**, 5175 (1973).

(10) V. G. Anicich and M. T. Bowers, *Int. J. Mass Spectrom. Ion Phys.*, **11**, 555 (1973); R. M. O'Malley, K. R. Jennings, M. T. Bowers, and V. G. Anicich, *ibid.*, **11**, 99 (1973).

(11) V. G. Anicich, Ph.D. Thesis, University of California at Santa Barbara, 1973.